

in the iron-containing samples. In all samples, some oxide formation was detected by the appearance of an Fe-Fe shell at 3.01 Å. The particle size of these clusters is estimated to be at least 6 Å; thus, it is very likely that they are located in the supercages rather than sodalite units. This could eliminate the site-directing effect of the second transition metal on the position of the Pd phases, and the effect on the reducibility is expected to be minimal.

This analysis shows that the interplay of metals in bimetallic zeolite catalyst is not easily predictable and is strongly dependent on the chemistry of each constituent. EXAFS is a valuable technique for structure determination of these complex systems by probing the ligand spheres of each component separately. On

the basis of subtle changes in zeolite oxygen coordination of the metal, it is demonstrated that EXAFS is also very sensitive for the analysis of intrazeolite reduction degrees.

**Acknowledgment.** Acknowledgment is made to the donors of the Petroleum Research Fund, administered by the American Chemical Society, and to the Sandia-University Research Program (DOE), for partial support of this research. The operational funds for NSLS beamline X-11A are supported by DOE Grant DE-AS0580ER10742.

**Registry No.** Pd, 7440-05-3; Fe, 7439-89-6; Co, 7440-48-4.

## Electrophoretic Light Scattering of Surfactant Micelle Colloids

Toyoko Imae,\*

Department of Chemistry, Faculty of Science, Nagoya University, Chikusa, Nagoya 464, Japan

William Otani, and Koichi Oka

Otsuka Electronics Company, Ltd., Hirakata, Osaka 573, Japan (Received: May 8, 1989;  
In Final Form: June 27, 1989)

Aqueous micellar solutions were investigated by the electrophoretic light scattering method. The electrophoretic mobilities of  $(2-4) \times 10^{-4} \text{ cm}^2 \text{ V}^{-1} \text{ s}^{-1}$  were obtained for charged micelles of tetradecyl- and hexadecyltrimethylammonium salicylates ( $\text{C}_{14}\text{TASal}$ ,  $\text{C}_{16}\text{TASal}$ ) and partly protonated tetradecyl- and oleyldimethylamine oxides ( $\text{C}_{14}\text{DAO}$  and  $\text{ODAO}$ ).

### Introduction

Electrophoretic light scattering is a beneficial method in which the electrophoretic mobility and the mutual diffusion coefficient can be measured simultaneously. Since the initial development of theory and experimental procedures by Ware and Flygare,<sup>1</sup> the technique has been applied to solutions of biomolecules, biocolloids, and polyelectrolytes and to suspensions of polymer latex particles and mineral colloidal particles.<sup>1-6</sup> However, applications to surfactant micelle colloidal systems have not been achieved as yet.

In the present paper, electrophoretic light scattering measurements were carried out for aqueous micellar solutions of  $\text{C}_{14}\text{TASal}$ ,  $\text{C}_{16}\text{TASal}$  and partly protonated  $\text{C}_{14}\text{DAO}$  and  $\text{ODAO}$ . The electrophoretic mobilities of charged micelles are obtained together with their mutual diffusion coefficients.

### Experimental Section

Samples of  $\text{C}_{14}\text{TASal}$  and  $\text{C}_{16}\text{TASal}$  were prepared by reacting the corresponding alkyltrimethylammonium halides with sodium salicylate in water. The preparation will be described in detail in a subsequent paper.<sup>7</sup> Samples of  $\text{C}_{14}\text{DAO}$  and  $\text{ODAO}$  are the same as those previously prepared and used.<sup>8,9</sup>  $\text{C}_{14}\text{DAO}$  and

$\text{ODAO}$  are weak bases and are partly protonated in the presence of HCl.

The electrophoretic mobility and the mutual diffusion coefficient were measured at 25 °C on Otsuka Electronics electrophoretic light scattering spectrophotometer, ELS-800. He-Ne laser light at 632.8 nm was used. The electrophoretic rectangular cell of  $2 \times 10 \times 17 \text{ mm}$  is separated by cellulose semipermeable membranes from the electrode chambers, which hold the Pt electrodes coated with Pt-black.

The electric field, which is perpendicular to the incident radiation, is applied in 1-s pulses that are reversed on each successive application. The sign of the electrophoretic mobility was determined by modulating the frequency of the reference light. The autocorrelation function of the dynamic light scattering was analyzed by a fast Fourier transform routine.

### Results

When the electric field,  $E$ , is applied to aqueous solutions of charged particles, the particles are moved by an electrophoretic drift velocity of  $v$ . Then, the electrophoretic mobility,  $U$ , is described as the velocity per unit electric field, that is

$$U = v/E \quad (1)$$

On the basis of the photon correlation method by the heterodyne mixing mode, the first-order autocorrelation power spectrum,  $F_1(\mu, \omega)$ , of the light scattered from the moving particles in solutions under the external electric field applied perpendicularly to the incident radiation is written by

$$F_1(\mu, \omega) = \frac{\langle N \rangle}{\pi} \frac{\mu^2 D}{(\omega + \mu \cdot v)^2 + (\mu^2 D)^2} \quad (2)$$

and

$$\mu \cdot v = \mu v \cos(\theta/2) \quad (3)$$

where  $\mu$  and  $\mu$  are the scattering vector and its magnitude, respectively;  $\omega$  is the angular frequency;  $\langle N \rangle$  is the average number of scatterers;  $D$  is the mutual diffusion coefficient; and  $\theta$  is a scattering angle. The power spectrum exhibits a Lorentzian peak

(1) Ware, B. R.; Flygare, W. H. *Chem. Phys. Lett.* **1971**, *12*, 81; *J. Colloid Interface Sci.* **1972**, *39*, 670.

(2) Urgiris, E. E. *Opt. Commun.* **1972**, *6*, 55; *Rev. Sci. Instrum.* **1974**, *45*, 74.

(3) Yoshimura, T.; Kikkawa, A.; Suzuki, N. *Jpn. J. Appl. Phys.* **1972**, *11*, 1979; *Jpn. J. Appl. Phys.* **1975**, *14*, 1853; *Opt. Commun.* **1975**, *15*, 277.

(4) Ware, B. R.; Haas, D. D. *Electrophoretic Light Scattering*. In *Fast Methods in Physical Biochemistry and All Biology*; Shāafi, R. I., Fernandeg, S. M., Eds.; Elsevier: New York, 1983; Chapter 8.

(5) Dalgleish, D. G. *J. Dairy Res.* **1984**, *51*, 425. Holt, C.; Dalgleish, D. *G. J. Colloids Interface Sci.* **1986**, *114*, 513.

(6) Dalbiez, J. P.; Tabti, K.; Darian, P. J.; Drifford, M. *Rev. Phys. Appl.* **1987**, *22*, 1013.

(7) Imae, T.; Hashimoto, K.; Ikeda, S. *Colloid Polym. Sci.*, in press.

(8) Abe, A.; Imae, T.; Shibuya, A.; Ikeda, S. *Surf. Sci. Technol.* **1988**, *4*, 67.

(9) Imae, T.; Ikeda, S. *J. Colloid Interface Sci.* **1984**, *98*, 363; *Colloid Polym. Sci.* **1985**, *263*, 756.

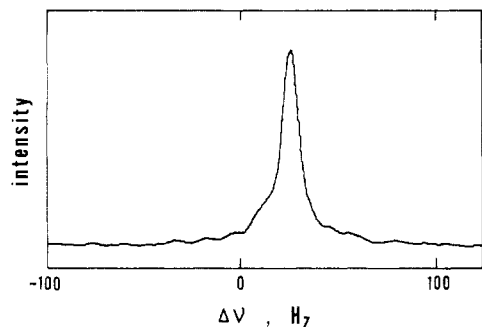


**Figure 1.** Power spectrum of aqueous  $C_{14}$ DAO solutions at a surfactant concentration of  $0.305 \times 10^{-2} \text{ g cm}^{-3}$  with 0.005 N HCl and 0.05 M NaCl at 25 °C represented as a function of the Doppler frequency:  $\theta = 10^\circ$ ;  $E = 31.7 \text{ V cm}^{-1}$ .

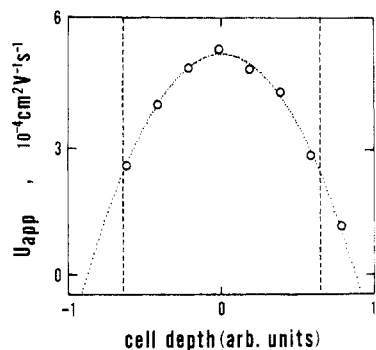


**Figure 2.** Cell depth dependence of the apparent mobility for aqueous  $C_{14}$ DAO solutions at a surfactant concentration of  $0.305 \times 10^{-2} \text{ g cm}^{-3}$  with 0.005 N HCl and 0.05 M NaCl at 25 °C:  $\theta = 10^\circ$ ;  $E = 31.7 \text{ V cm}^{-1}$ ; ---, fitting curve; --, stationary level.

with a half-width,  $\Delta\omega_{1/2} = \mu^2 D$ , at half-height, the maximum of which is Doppler-shifted by  $\Delta\omega_{\text{shift}} = \mu v \cos(\theta/2)$  from the spectrum peak obtained when the electric field is not applied.

The power spectrum of aqueous  $C_{14}$ DAO solutions at a surfactant concentration,  $c$ , of  $0.305 \times 10^{-2} \text{ g cm}^{-3}$  with 0.005 N HCl and 0.05 M NaCl at 25 °C is represented as a function of the Doppler frequency in hertz,  $\Delta\nu = \Delta\omega/2\pi$ , in Figure 1. The spectrum, which was measured at a scattering angle of  $10^\circ$  under the electric field of  $31.7 \text{ V cm}^{-1}$ , displays a single peak, but the peak position or the apparent mobility changes with a cell depth, as seen in Figure 2. This observation is due to the effect of the electroosmosis caused by the electric charge on the wall of the electrophoretic quartz cell.

Although correction for electroosmosis has not been firmly established in earlier work,<sup>1-3,5</sup> it is clear from Figure 2 that electroosmosis may become a dominant phenomenon in electrophoresis experiments. Thus, in order to correct this effect, the apparent mobilities,  $U_{\text{app}}$ , were measured at different positions along the depth axis of the cell wall, and the true mobility at the stationary level was evaluated, by fitting the observed data to the theoretical equation of Mori and Okamoto.<sup>10</sup> A mobility value of  $2.33 \times 10^{-4} \text{ cm}^2 \text{ V}^{-1} \text{ s}^{-1}$  was obtained for aqueous  $C_{14}$ DAO solutions described above.

The same procedure was applied to other systems examined in this paper, and the obtained numerical values of the electrophoretic mobilities are listed in Table I with experimental conditions and numerical values of other parameters. The electrophoretic mobilities of  $(2-4) \times 10^{-4} \text{ cm}^2 \text{ V}^{-1} \text{ s}^{-1}$  were obtained for charged micelles of  $C_{14}$ TASal,  $C_{16}$ TASal,  $C_{14}$ DAO, and ODAO.

Table I also includes numerical values of the mutual diffusion coefficient,  $D$ , and the apparent hydrodynamic radius,  $R_H$ , which were evaluated by cumulant analysis on the dynamic light scattering measurement of homodyne mode without the electric field. Since the apparent hydrodynamic radii are larger than the radii of spherical micelles,<sup>11</sup> rodlike micelles must be formed in aqueous

**TABLE I: Electrophoretic Light Scattering Data of Charged Micelles at 25 °C**

| $10^2 c$ ,<br>$\text{g cm}^{-3}$            | $\theta$ ,<br>deg | $E$ ,<br>$\text{V cm}^{-1}$ | $10^2 v$ ,<br>$\text{cm s}^{-1}$ | $10^4 U$ ,<br>$\text{cm}^2 \text{ V}^{-1} \text{ s}^{-1}$ | $10^7 D$ ,<br>$\text{cm}^2 \text{ s}^{-1}$ | $R_H$ ,<br>nm |
|---|-------------------|-----------------------------|----------------------------------|---|--|---------------|
| $C_{14}$ TASal in Water                     |                   |                             |                                  |   |  |               |
| 0.188                                       | 10                |                             |                                  |   | 3.35                                       | 7.3           |
| 0.388                                       | 10                | 90                          | 2.26                             | 2.51  | 3.75                                       | 6.6           |
| 0.774                                       | 10                | 89                          | 1.84                             | 2.07  | 5.17                                       | 4.8           |
| $C_{16}$ TASal in Water                     |                   |                             |                                  |   |  |               |
| 0.055                                       | 10                | 49.8                        | 2.16                             | 4.34  | 0.370                                      | 66.1          |
| $C_{14}$ DAO in 0.005 N HCl and 0.05 M NaCl |                   |                             |                                  |   |  |               |
| 0.305                                       | 10                | 31.7                        | 0.74                             | 2.33  | 0.972                                      | 25.2          |
| $C_{14}$ DAO in 0.005 N HBr and 0.01 M NaBr |                   |                             |                                  |   |  |               |
| 0.303                                       | 10                | 47.8                        | 1.32                             | 2.75  | 1.16                                       | 21.1          |
| ODAO in 0.001 N HCl                         |                   |                             |                                  |   |  |               |
| 0.118                                       | 5                 | 64.6                        | 2.47                             | 3.83  | 0.766                                      | 32.1          |
| ODAO in 0.001 N HCl and 0.01 M NaCl         |                   |                             |                                  |   |  |               |
| 0.118                                       | 10                | 45.2                        | 1.43                             | 3.17  | 0.412                                      | 61.0          |

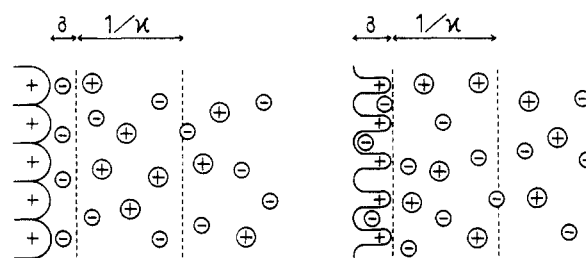


**Figure 3.** Models of the electric surface structure of charged micelles: left, smooth-surface model; right, rough-surface model;  $\delta$ , thickness of Stern layer;  $1/\kappa$ , Debye length.

surfactant solutions examined here. The formation of rodlike micelles of  $C_{14}$ TASal and  $C_{16}$ TASal in water and of ODAO in 0.001 N HCl and in 0.001 N HCl + 0.01 M NaCl was already confirmed.<sup>9,12</sup> It should be noted that the electrophoretic mobility is not necessarily related to the apparent hydrodynamic radius.

## Discussion

Stigter et al.<sup>13,14</sup> suggested that the surface of charged micelles is not smooth but rough. The electric surface structure of micelles as represented in Figure 3 is characterized by the electrostatic potentials at the micelle surface and at the Stern layer surface, which are related to the surface charge and the degree of ionization, while the electrophoretic mobility is concerned with the  $\zeta$  potential at the sliding plane, which is sometimes approximated to be the potential at the surface of the Stern layer.

The electrophoretic mobility of surfactant micelles was measured by a tracer electrophoretic method,<sup>13,15</sup> its modification,<sup>16</sup> and a Schlieren electrophoretic method.<sup>17-19</sup> The mobilities of charged micelles of sodium dodecyl sulfate, alkylammonium chlorides, alkyltrimethylammonium salts, dodecylpolyoxyethylene sulfate salts, dodecyltrimethylamine oxide, and (*N*-dodecyl- $\beta$ -amino)propionic acid were affected by salt concentration, temperature, the counterion species, the added-salt species, and pH.

Although the surface potentials, the surface charge, and the degree of ionization of charged spherical micelles were evaluated and discussed, by use of the observed electrophoretic mobili-

(11) Imae, T. *J. Colloid Interface Sci.* **1989**, *127*, 256.

(12) Rehage, H.; Hoffmann, H. *Faraday Discuss. Chem. Soc.* **1983**, *76*, 363.

(13) Stigter, D.; Mysels, K. J. *J. Phys. Chem.* **1955**, *59*, 45.

(14) Stigter, D. *J. Phys. Chem.* **1964**, *68*, 3603.

(15) Hoyer, H. W.; Greenfield, A. *J. Phys. Chem.* **1957**, *61*, 735.

(16) Sepúlveda, L.; Cortés, J. *J. Phys. Chem.* **1985**, *89*, 5322.

(17) Nakagawa, T.; Inoue, H. *Nippon Kagaku Zasshi* **1957**, *78*, 636.

(18) Tokiwa, F. *J. Phys. Chem.* **1968**, *72*, 4331; *Nippon Kagaku Zasshi* **1969**, *90*, 1057.

(19) Tokiwa, F.; Ohki, K. *Bull. Chem. Soc. Jpn.* **1968**, *41*, 2828; *Bull. Chem. Soc. Jpn.* **1969**, *42*, 1216.

(10) Mori, S.; Okamoto, H. *Floatation* **1980**, *27*, 117.

ty,<sup>13,14,16-19</sup> the procedure was based on the theory for spherical particles. Such a procedure is not valid for the rodlike micelles concerned in this paper. If the precise theory is applied and the numerical values of appropriate parameters are evaluated, the electric surface properties of charged rodlike micelles will be

elucidated and then they may be compared with those of spherical micelles.

**Registry No.** C<sub>14</sub>TASal, 86996-35-2; C<sub>16</sub>TASal, 61482-44-8; C<sub>14</sub>DAO, 3332-27-2; ODAO, 14351-50-9.

## Small-Angle Neutron-Scattering Study of Triglyceride Solubilization by Lecithin Micelles: A Direct Observation of Rod-to-Sphere Transition

Tsang-Lang Lin,<sup>\*,†</sup> Sow-Hsin Chen,<sup>†</sup> N. Elise Gabriel,<sup>‡</sup> and Mary F. Roberts<sup>‡§</sup>

Department of Nuclear Engineering, National Tsing-Hua University, Hsin-Chu, Taiwan 30043, ROC  
(Received: May 10, 1989; In Final Form: August 16, 1989)

The solubilization of tributyrin by rodlike diheptanoylphosphatidylcholine (diheptanoyl-PC) micelles has been studied by small-angle neutron-scattering techniques. A rod to sphere transition is observed from the measured angular distribution of neutron-scattering intensities. The transition is from the rodlike micelle to a globular mixed micelle which has tributyrin molecules at the core surrounded by an outer shell of diheptanoyl-PC molecules. When the molar ratio of tributyrin to diheptanoyl-PC is increased beyond 0.18, all rodlike diheptanoyl-PC micelles are transformed into globular mixed micelles. The size of these globular mixed micelles increases with increasing tributyrin concentration in the simple micelle region up to the solubility limit. The small-angle neutron scattering data were analyzed to obtain the structural parameters of the mixed micelles. It is found that the growth of the mixed micelles does not follow a constant available surface area model or a constant palisade layer thickness model. If the model is modified to include tributyrin molecules at the surface of the mixed micelle, the growth behavior can be explained. For the tributyrin/diheptanoyl-PC molar ratio less than 0.18, rodlike micelles are found to coexist with globular mixed micelles. By fitting the neutron scattering data in the middle  $Q$  range, it is possible to determine the size and number density of the mixed micelles in the coexistence region. The results of analyzing the small-angle neutron scattering data in the coexistence region show that some tributyrin molecules are solubilized by the rodlike diheptanoyl-PC micelles and only part of the added tributyrin forms globular micelles. These globular mixed micelles, in coexistence with rodlike micelles, do not grow with increasing tributyrin concentration, in contrast to the results found in the simple mixed micelle region.

### Introduction

Short-chain lecithins (with 12-16 carbons in the fatty acyl chains) form micelles in aqueous solutions.<sup>1</sup> The size distribution of these particles depends on the fatty acyl chain length. Dihexanoylphosphatidylcholine (dihexanoyl-PC) forms globular micelles with a critical micellar concentration of about 15 mM.<sup>2</sup> The size and structure of dihexanoyl-PC micelles are unchanged over a large concentration range.<sup>2,3</sup> Diheptanoylphosphatidylcholine (diheptanoyl-PC), which has an additional methylene group on each chain, has a cmc of 1.5 mM and forms rodlike micelles at relatively low concentrations.<sup>4</sup> The average length of the rodlike diheptanoyl-PC micelles increases rapidly with increasing lipid concentration. The size distribution of these polydisperse micelles at a given concentration has been characterized by small-angle neutron scattering techniques.<sup>4</sup> Asymmetric linear short-chain lecithins also form polydisperse rodlike micelles.<sup>5</sup> A thermodynamic model has been presented to explain the formation and growth of the rodlike micelles.<sup>4</sup> Globular micelles can grow into rodlike micelles only when the gain in free energy upon incorporating an additional monomer overcomes the unfavorable decrease in entropy. The gain in free energy comes from the fact that the rodlike micelles have smaller surface area per molecule in contact with water as compared with the case of globular micelles.

Solubilization of oil by micellar surfactant solutions has been an important area of research with applications in a wide variety of fields.<sup>6-9</sup> As a specific example in the area of biochemistry, micelles of short-chain lecithins have been shown to solubilize relatively large amounts of triglycerides.<sup>8,10</sup> The mixed micelles produced are biological models for lipoproteins and excellent substrates for a variety of water-soluble lipases.<sup>8,10</sup> It has been suggested by quasi-elastic light-scattering (QELS) measurements that rodlike lecithin micelles can be transformed into globular mixed micelles by solubilization of additives, which are typically apolar or only weakly hydrophilic.<sup>8</sup> It was observed that when the additive reaches a certain concentration, all the rodlike micelles are transformed into globular mixed micelles. The maximum amount of additive that can be solubilized by a given amount of surfactant depends on both the specific type of additive as well as the surfactant system. For diheptanoyl-PC micelles, the maximum amount of tributyrin that can be solubilized is 36 mol % of the PC concentration.<sup>8</sup> It was proposed that, at low tri-

\* Correspondence should be addressed to Dr. Tsang-Lang Lin at the Department of Nuclear Engineering, National Tsing-Hua University, Hsin-Chu, Taiwan 30043, ROC.

† Department of Nuclear Engineering, and the Center for Materials Science and Engineering, Massachusetts Institute of Technology, Cambridge, MA 02139.

‡ Department of Chemistry, Massachusetts Institute of Technology, Cambridge, MA 02139.

§ Present address: Department of Chemistry, Boston College, Chestnut Hill, MA 02167.

(1) Tausk, R. J. M.; Karmiggelt, J.; Oudshoorn, C.; Overbeek, J. Th. G. *Biophys. Chem.* **1974**, *1*, 175.

(2) Lin, T.-L.; Chen, S.-H.; Gabriel, N. E.; Roberts, M. F. *J. Am. Chem. Soc.* **1986**, *108*, 3499.

(3) Burns, Jr., R. A.; Roberts, M. F.; Dluhy, R.; Mendelsohn, R. *J. Am. Chem. Soc.* **1982**, *104*, 430.

(4) Lin, T.-L.; Chen, S.-H.; Gabriel, N. E.; Roberts, M. F. *J. Phys. Chem.* **1987**, *91*, 406.

(5) Lin, T.-L.; Chen, S. H.; Roberts, M. F. *J. Am. Chem. Soc.* **1987**, *109*, 2321.

(6) Carroll, B. J. *J. Chem. Soc., Faraday Trans.* **1986**, *82*, 3205.

(7) Stecker, M. M.; Benedek, G. B. *J. Phys. Chem.* **1984**, *88*, 6519.

(8) Burns, Jr., R. A.; Donovan, J. M.; Roberts, M. F. *Biochemistry* **1983**, *22*, 964.

(9) Chaiko, M. A.; Nagarajan, R.; Ruckenstein, E. *J. Colloid Interface Sci.* **1984**, *99*, 181.

(10) Burns, R. A.; Roberts, M. F.; *J. Biol. Chem.* **1981**, *256*, 2716.